The Effect of Vibration Frequency on the Effective Mass Spin Splitting of Polaron in a Parabolic Quantum Well

S.-P. Shan*, W. Liu, W.-D. Zou,
R.-X. Chen and C. Hu

College of Physics and Electromechanics, Longyan University, Longyan, 364012, No. 1 Dongxiao North Road, Longyan, 364012, China

Received: 31.08.2023 & Accepted: 18.01.2024

Doi: 10.12693/APhysPolA.145.157 *e-mail: ssping04@126.com

Using Tokuda's improved linear combination operator method and variational technique, the expression of the polaron effective mass in a parabolic quantum well is derived. Due to the spin–orbit interaction, the effective mass ratio of polaron splits into two branches. The dependence of the effective mass ratio on the vibration frequency, the spin–orbit coupling parameter, and the velocity is discussed by numerical calculation in the presence and absence of phonon. The effective mass ratio of polaron is an increasing function of vibration frequency. The absolute value of the spin splitting effective mass ratio increases with the increase in the spin–orbit coupling parameter and decreases with the increase in velocity. Due to the heavy hole characteristic of spin–orbit interaction, the spin splitting effective mass ratio is negative. The effective mass ratio is larger in the presence of a phonon than in the absence of a phonon, and the effective mass ratio splitting distance is independent of the phonon.

topics: parabolic quantum well, effective mass spin splitting, vibration frequency, heavy hole characteristic

1. Introduction

Since 1988, researchers have done extensive research on spintronics and have achieved a great deal of research results [1, 2]. Spintronics has important research value, which can help people understand the microscopic world and can promote the research and development of new electronic devices. It has become an active research area for condensed matter physics due to the potential influence on information technology and many interesting problems of its own. If the inversion symmetry of the crystal structure is broken, the electron will experience spin splitting. The Rashba spin–orbit splitting due to the asymmetry of the structure inversion is dominant in the narrow gap semiconductor electron spin splitting. In the past, people always thought that the source of the Rashba effect was caused by the electric field at the heterojunction interface. However, theory and practice have proved that the contribution of the interface electric field is very small, and the main contribution comes from the penetration of the wave function at the barrier and the asymmetry at the interface.

In 1990, Datta et al. [3] first proposed the principle of transistors based on controlling the spin of electrons. Since the publication of Datta's article [3], many scholars around the world have carried out experimental and theoretical research work on the Rashba effect in low-dimensional quantum systems [4–7], especially in quantum well systems. For example, Li et al. [8] adopted the framework of effective-mass envelope function theory and investigated theoretically the Rashba spin–orbit splitting of a hydrogenic donor impurity in GaAs/GaAlAs quantum wells. Using Kane's 8-band $\boldsymbol{k}\cdot\boldsymbol{p}$ theory and the envelope function approximation, Stanley et al. [9] derived a tight binding Hamiltonian for III–V semiconductor quantum well structures, which accurately models band structure and spin–orbit coupling. By applying a potential difference in the well, they calculated the Rashba spin–orbit splitting in the lowest conduction band. Rashba spin–orbit splitting in the asymmetric quantum wells with different growth orientations and electron densities was explored by Jin et al. [10]. The strong Rashba effect presented in the highly asymmetric quantum wells provides a potential candidate for spintronic devices. It is not difficult to find that people have done a lot of research work on the Rashba effect in the electronic system, and a few people have done research on it in the field of polaron. For example, one of the authors of the paper [11] used the Lee–Low–Pines (LLP) variational method to study the Rashba effect of polaron in a triangular quantum well. The influence of the Rashba effect on the ground state energy of polaron in a parabolic quantum well was also studied using the same method. The Rashba spin–orbit interaction led to the splitting of polaron ground state energy [12].

In this paper, the influence of Rashba spin–orbit interaction on the effective mass of polaron in a parabolic quantum well is studied using the unitary transformation and Tokuda's improved linear combination operator methods. The expression of the effective mass of the polaron is derived theoretically, and the effect of Rashba spin–orbit interaction on the effective mass of the polaron is discussed by numerical calculation.

2. Theoretical derivation

A parabolic quantum well composed of two polar materials grows in the z-direction, and electron motion is strongly restricted in the growth direction compared to the other two directions. Under the influence of Rashba spin–orbit interaction, the Hamiltonian of the electron–phonon system in a parabolic quantum well is

$$\begin{aligned} H = {} & \frac{p_{\parallel}^2}{2m} + \frac{p_z^2}{2m} + V(z) + \sum_{q} \hbar\omega_{LO}\, a_{\boldsymbol{q}}^{+} a_{\boldsymbol{q}} \\ & + \sum_{q} \left[V_q\, a_{\boldsymbol{q}} \exp(\mathrm{i}\boldsymbol{q}\cdot\boldsymbol{r}) + \mathrm{h.c.} \right] \\ & + \mathrm{i}\frac{\alpha_{\mathrm{R}}}{2\hbar^3} \left(\hat{p}_{-}^3 \hat{\sigma}_{+} - \hat{p}_{+}^3 \hat{\sigma}_{-} \right). \end{aligned} \tag{1}$$

In (1), $p_{\pm} = p_x \pm \mathrm{i}p_y$, $\sigma_{\pm} = \sigma_x \pm \sigma_y$; p and σ are the momentum of the electron and the Pauli operator, respectively; $a_{\boldsymbol{q}}^{+}$ ($a_{\boldsymbol{q}}$) is the creation (annihilation) operator of the bulk longitudinal optical phonon with the wave vector $\boldsymbol{q}$ and frequency ω_{LO}; $\boldsymbol{r} = (\boldsymbol{\rho}, z)$ represents the coordinate vector of a single electron. The last term in (1) represents the Hamiltonian that only considers band splitting of heavy-hole states in the spin–orbit coupling effect. The third term in (1) represents the confined potential energy of the polaron, which is

$$V(z) = \begin{cases} V_0 \left(\frac{z}{d}\right)^2, & |z| \le d, \\ V_0, & |z| > d, \end{cases} \tag{2}$$

and the quantity V_q in (1) can be expressed as

$$V_q = \mathrm{i} \left(\frac{\hbar\omega_{LO}}{q} \right) \left(\frac{\hbar}{2m\omega_{LO}} \right)^{1/4} \left(\frac{4\pi\alpha}{V} \right)^{1/2}. \tag{3}$$

In (2), α and V are defined as the electron–phonon coupling strength and the crystal volume, respectively. In (3), V_0 and d are defined as the well depth and the well width, respectively.

An improved linear combination operator is introduced for the momentum and the coordinate of the moving electron in the x–y plane [13]

$$\begin{aligned} p_j &= \sqrt{\frac{m\hbar\lambda}{2}} \left(b_j + b_j^{+} + p_{0j} \right), \\ r_j &= \mathrm{i}\sqrt{\frac{\hbar}{2m\lambda}} \left(b_j - b_j^{+} \right). \end{aligned} \tag{4}$$

Here, $j = x, y$; λ and p_{0j} are variational parameters, and λ also represents the vibrational frequency of polaron. By substituting the linear combination operator into (1) and performing the second unitary transformation on it, we take the following unitary transformation operator

$$U = \exp\left[\sum_{q} \left(f_q a_{\boldsymbol{q}}^{+} - f_q^{*} a_{\boldsymbol{q}} \right) \right]. \tag{5}$$

Here, f_q (f_q^{*}) is a variational parametric function. The unitary transformed Hamiltonian is

$$H' = H_0' + \frac{p_z^2}{2m}, \tag{6}$$

where

$$\begin{aligned} H_0' = {} & \frac{\hbar\lambda}{4} \sum_j \left(b_j^{+} b_j^{+} + b_j b_j \right) + \frac{\hbar\lambda}{2} \sum_j \left(b_j^{+} b_j + 1 \right) + \frac{\hbar\lambda p_0^2}{4} + \frac{\hbar\lambda}{2} \sum_j \left(b_j + b_j^{+} \right) p_{0j} + \sum_q \hbar\omega_{LO} \left(a_{\boldsymbol{q}}^{+} + f_q^{*} \right) \left(a_{\boldsymbol{q}} + f_q \right) \\ & + \sum_q \left\{ V_q \left(a_{\boldsymbol{q}} + f_q \right) \exp\left(-\frac{\hbar q^2}{4m\lambda} \right) \exp\left[-\sqrt{\frac{\hbar}{2m\lambda}} \sum_j b_j^{+} q_j \right] \exp\left[\sqrt{\frac{\hbar}{2m\lambda}} \sum_j b_j q_j \right] + \mathrm{h.c.} \right\} \\ & + V_0 \left(\frac{z}{d} \right)^2 \pm \frac{\alpha_{\mathrm{R}}}{\hbar^3} \left(\frac{m\hbar\lambda}{2} \right)^{3/2} \left(p_0^3 - p_0 \right). \end{aligned} \tag{7}$$

In (7), $p_0^2 = p_{0x}^2 + p_{0y}^2$. Let the ground state trial wave function of the system be

$$\begin{aligned} |\Psi_0\rangle &= |\varphi(z)\rangle \left(c\, \chi_{1/2} + d\, \chi_{-1/2} \right) |0\rangle_a |0\rangle_0, \\ \varphi(z) &= \left(\frac{2\beta}{\pi} \right)^{1/4} \exp\left(-\beta z^2 \right), \end{aligned} \tag{8}$$

where $|\varphi(z)\rangle$ is the wave function of the electron in the z-direction, which satisfied $\langle\varphi(z)|\varphi(z)\rangle = \delta$; δ is Kronecker delta symbol; $|0\rangle_a$ and $|0\rangle_b$ are the polaron ground state and the zero phonon state, respectively. In order to obtain the effective mass of the polaron, the variational function $J = H_0' - U^{-1}(\boldsymbol{u}\cdot\boldsymbol{P}_{\parallel T})$ is introduced, and its mean value in the $|\Psi_0\rangle$ state is calculated as

$$F(\lambda, u, p_0, f_q) = \left\langle \psi_0 \left| H_0' - U^{-1} \left(\boldsymbol{u}\cdot\boldsymbol{P}_{\parallel T} \right) U \right| \psi_0 \right\rangle. \tag{9}$$

The Lagrange multiplier is $\boldsymbol{u}$, which represents the average velocity of the electron.

Here,

$$\boldsymbol{P}_{\parallel T} = \boldsymbol{p}_{\parallel} + \sum_{q} a_{\boldsymbol{q}}{}^{+} a_{\boldsymbol{q}}\, \hbar \boldsymbol{q}_{\parallel} \tag{10}$$

is the total momentum of the system in the plane, and $\boldsymbol{p}_{\parallel}$ is the momentum operator of the electron in the plane.

Performing $\frac{\partial F}{\partial f_q} = 0$ and $\frac{\partial F}{\partial f_q^*} = 0$, we get, respectively,

$$f_q^* = -\frac{V_q}{\hbar\omega_{LO} - \hbar\,\boldsymbol{u}\cdot\boldsymbol{q}}\ \exp\left(-\frac{\hbar}{4m\lambda}q^2\right) \tag{11}$$

and

$$f_q = -\frac{V_q^*}{\hbar\omega_{LO} - \hbar\,\boldsymbol{u}\cdot\boldsymbol{q}}\exp\left(-\frac{\hbar}{4m\lambda}q^2\right). \tag{12}$$

By substituting f_q and f_q^* into (9) and replacing the sum with an integral, we get

$$F(\lambda, p_0, u) = \frac{\hbar\lambda}{4}p_0^2 + \frac{\hbar\lambda}{2} + \frac{V_0}{4\beta d^2} - \frac{\alpha\hbar}{2}\sqrt{\omega_{LO}\pi\lambda}$$
$$-\frac{\alpha u^2 m\sqrt{\pi}}{4}\left(\frac{\lambda}{\omega_{LO}}\right)^{3/2} - u\left(\frac{m\hbar\lambda}{2}\right)^{1/2} p_0$$
$$\pm\frac{\alpha_{\mathrm{R}}}{\hbar^3}\left(\frac{m\hbar\lambda}{2}\right)^{3/2}\left(p_0^3 - p_0\right). \tag{13}$$

Now, we ignore p_0^3. Using the variational method, p_0 is obtained and substituted into (13). Then, we take the variation of F with respect to λ, and the expression of the vibration frequency of the polaron can be obtained by taking the extreme value. The vibration frequency λ satisfies

$$\frac{\hbar}{2} - \frac{\alpha\hbar}{4}\sqrt{\frac{\omega_{LO}\pi}{\lambda}} - \frac{3}{8}\alpha u^2\sqrt{\pi}m\frac{\sqrt{\lambda}}{\omega_{LO}^{3/2}} = 0. \tag{14}$$

By solving (14), we get the polaron vibration frequency λ_0. From (13), the effective mass of polaron can be expressed as

$$m^* = \left[1 + \frac{\alpha\sqrt{\pi}}{2}\left(\frac{\lambda}{\omega_{LO}}\right)^{3/2} \pm \left(-\frac{\alpha_{\mathrm{R}} m\lambda}{\hbar^2 u}\right)\right] m. \tag{15}$$

The material has anisotropy, and the effective mass is different in all directions. However, in (15), we calculate the mean effective mass of the polaron rather than the effective mass along one of the crystallographic axes of the lattice.

3. Numerical calculation and result discussion

In order to investigate the influence of vibration frequency on the effective mass spin splitting of polaron in a parabolic quantum well, the effective mass ratio of the polaron is calculated numerically, and the changes in effective mass ratio with the vibration frequency, the velocity, and the spin–orbit coupling parameter are discussed. At the same time, the relations among the spin splitting effective mass ratio with the velocity and the spin–orbit coupling parameter are also discussed. We take RbCl as an example material and perform the numerical calculations. The corresponding parameters for RbCl are $m = 0.432m_0$, $\omega_{LO} = 3.39 \times 10^{13}$ s^{-1}, $\alpha = 4.2$. Here, m_0 is the free electron mass. The numerical results are shown in Figs. 1–5. In Figs. 1–4, we use a solid line to represent the effective mass ratio of zero spin splitting m_0^*/m, a short solid line to stand for the effective mass ratio of spin-up splitting m_+^*/m, and dotted lines to mark the effective mass ratio of spin-down splitting m_-^*/m.

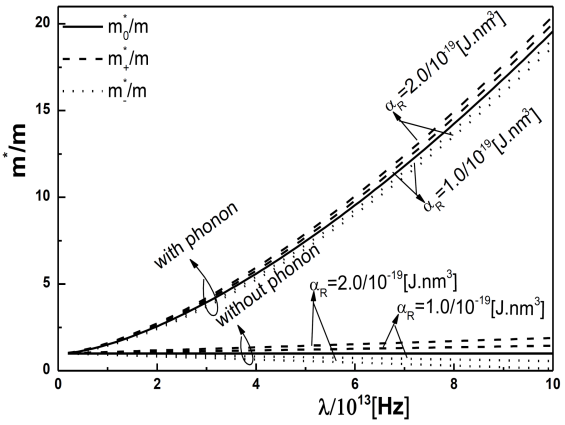

Fig. 1. The relational curve between the effective mass ratio m^*/m and the vibration frequency λ with phonon and without phonon at different spin–orbit coupling parameters α_{R}.

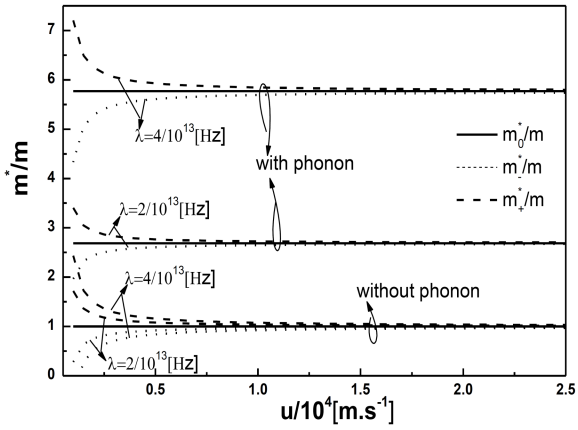

Fig. 2. The relational curve between the effective mass ratio m^*/m and the velocity u with phonon and without phonon at different vibration frequencies λ.

When the spin–orbit coupling parameters are assigned values of 1.0×10^{-19} J nm^3 and 2.0×10^{-19} J nm^3, respectively, Fig. 1 shows the relationship between the polaron effective mass ratio m^*/m and the vibration frequency λ with phonon and without phonon. In the figure, we find that the effective mass ratio splits into two branches on the basis of zero spin in both cases with phonon and without phonon, and the splitting distance increases with the increase in the polaron vibration frequency.

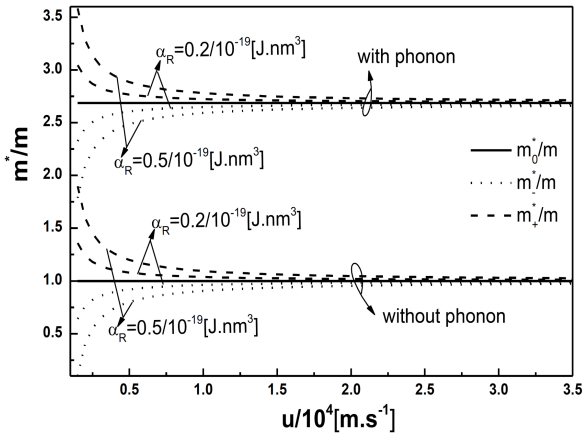

Fig. 3. The relational curve between the effective mass ratio m^*/m and the velocity u with phonon and without phonon at different spin–orbit coupling parameters $\alpha_{\rm R}$.

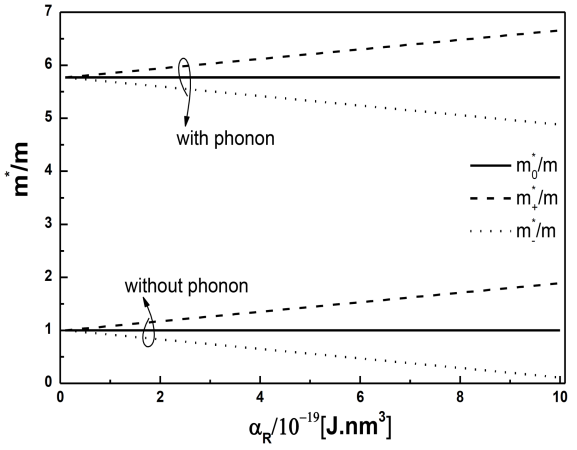

Fig. 4. The relational curve between the effective mass ratio m^*/m and the spin–orbit coupling parameter $\alpha_{\rm R}$ with phonon and without phonon.

This splitting is caused by the spin–orbit interaction due to the asymmetric structure of the parabolic quantum well. From (15), it can be seen that the vibration frequency of polaron is directly proportional to the effective mass spin splitting, which is consistent with the conclusion from Fig. 1. We also find from Fig. 1 that the polaron effective mass ratio increases significantly with the increase in vibration frequency in the presence of phonon. Since the increase in vibration frequency leads to the enhancement of electron–phonon interaction, the effective mass ratio of polaron increases with the increase in vibration frequency. However, the effective mass ratio of zero spin splitting is constant when phonons are ignored. When electron–phonon coupling strength $\alpha = 0$, from (15), we get the expression $m^*/m = 1$ for the effective mass ratio of zero spin splitting. In the absence of phonon, one can see that the effective mass ratio changes linearly with the increase in vibration frequency. However,

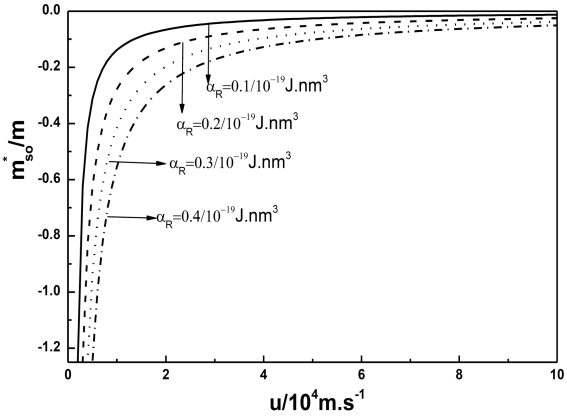

Fig. 5. The relational curve between the spin splitting effective mass ratio m_{so}^*/m and the velocity u at different spin–orbit coupling parameters $\alpha_{\rm R}$.

in the presence of phonon, the effective mass ratio changes parabolically with the increase in vibration frequency.

When the vibration frequencies are taken as $\lambda = 2 \times 10^{13}$ Hz and $\lambda = 4 \times 10^{13}$ Hz, respectively, the result in Fig. 2 shows the relations between the effective mass ratio m^*/m and the velocity u of the polaron with phonon and without phonon. Figure 3 displays the relationship between the effective mass ratio m^*/m and the velocity u of the polaron with phonon and without phonon, considered for fixed $\alpha_{\rm R} = 0.2{\times}10^{-19}$ J nm^3 and $\alpha_{\rm R} = 0.5{\times}10^{-19}$ J nm^3. From Figs. 2 and 3, it is found that the two branches of the polaron effective mass ratio show the opposite trend with the increase in the velocity. That is to say, the spin-up effective mass ratio is a decreasing function of velocity, while the spin-down effective mass ratio is an increasing function of velocity. This is because the velocity in (15) is inversely proportional to the effective mass of spin splitting. When $u < 1.0 \times 10^4$ m/s, the splitting distance increases rapidly as the velocity decreases. When $u > 1.0 \times 10^4$ m/s, as the velocity increases, the splitting distance slowly decreases and tends to zero. It can be seen that the larger the vibration frequency, the more significant the effective mass ratio splitting is. The conclusion is consistent with Fig. 1.

Figure 4 describes the relational curve between the effective mass ratio m^*/m and the Rashba spin–orbit parameter $\alpha_{\rm R}$ with phonon and without phonon. The figure shows that the effective mass ratio of zero spin–orbit interaction does not change with the increase in the Rashba spin–orbit parameter. However, the splitting distance increases with the increase in the Rashba spin–orbit parameter. Since the spin–orbit coupling parameter is linearly related to the spin splitting effective mass ratio, the larger the spin–orbit coupling parameter is, the larger the splitting distance will be. This conclusion is consistent with Figs. 1 and 3. Figures 1–4 have a common feature that the effective mass ratio is

larger in the presence of a phonon than in the absence of a phonon, and the effective mass ratio splitting distance is independent of the phonon. Because the phonon field around the electron interacts with the electron to form a polaron, the mass of the polaron is greater than that of the electron.

Figure 5 shows the relationship between the spin splitting effective mass ratio m^*_{so}/m and the velocity u when the spin–orbit coupling parameter takes different values. Figure 5 shows that the absolute value of the spin splitting effective mass ratio is an increasing function of the spin–orbit coupling parameter but a decreasing function of velocity. This indicates that the spin–orbit coupling parameter has a positive effect on the spin splitting effective mass ratio, while the velocity has a negative effect on the spin splitting effective mass ratio. When $u < 1 \times 10^4$ m/s, the absolute value of the spin splitting effective mass ratio increases sharply with the decrease in the velocity. Outside this range, the spin splitting effective mass ratio changes slowly with the change in the velocity. At the range of $1.5 \times 10^4 < u < 3 \times 10^4$ m/s, different spin–orbit coupling parameters have a great influence on the spin splitting effective mass ratio. An important phenomenon is found in Fig. 5, where the spin splitting effective mass ratio is negative. It is caused by the heavy hole characteristic of spin–orbit splitting.

4. Conclusions

The influence of vibration frequency on the effective mass spin splitting of polaron in a parabolic quantum well is studied theoretically. Under the influence of the Rashba effect, the effective mass of the polaron splits into two branches on the basis of zero spin. The effective mass ratio increases with the increase in vibration frequency. The effective mass ratio splitting distance increases with the increase in vibration frequency and spin–orbit coupling parameter, and decreases with the increase in velocity. We obtain an interesting conclusion that the spin splitting effective mass ratio is negative. This is because spin–orbit coupled splitting only takes into account the splitting of the heavy-hole band, so the spin splitting effective mass ratio is negative. The effective mass ratio is larger in the presence of a phonon than in the absence of a phonon, and the effective mass ratio splitting distance is independent of the phonon.

Acknowledgments

This work was funded by the Natural Science Foundation of Fujian Province (2020J05199) and Dr. Start Funding from Longyan University (LB2020005).

References

[1] E.I. Rashba, AI.L. Efros, *Phys. Rev. Lett.* **91**, 126405 (2003).

[2] S.A. Wolf, D.D. Awschalom, R.A. Buhrman, J.M. Daughton, S. von Molnár, M.L. Roukes, A.Y. Chtchelkanova, D.M. Treger, *Science* **294**, 1488 (2001).

[3] S. Datta, B. Das, *Appl. Phys. Lett.* **56**, 665 (1990).

[4] J. Lee, H.N. Specror, *J. Appl. Phys.* **99**, 113708 (2006).

[5] A.M. Babayev, S. Cakmaktepe, D. Turkoz Altug, *J. Phys. Conf. Ser.* **153**, 012043 (2009).

[6] J.P. Stanley, N. Pattinson, C.J. Lambert, J.H. Jefferson, *Physica E* **20**, 433 (2004).

[7] P. Mokhtari, G. Rezaei, A. Zamani, *Superlattices Microstruct.* **106**, 1 (2017).

[8] S.-S. Li, J.-B.Xia, *Appl. Phys. Lett.* **92**, 022102 (2008).

[9] J.P. Stanley, N. Pattinson, C.J. Lambert, J.H. Jefferson, *Physica E* **20**, 433 (2004).

[10] S. Jin, H. Wu, T. Xu, *Appl. Phys. Lett.* **95**, 132105 (2009).

[11] S.-P. Shan, S.-H. Chen, *J. Low Temp. Phys.* **197**, 379 (2019).

[12] S.-P. Shan, S.-H. Chen, *Iran. J. Sci. Technol. Trans. A Sci.* **41**, 755 (2017).

[13] N. Tokuda, *J. Phys. C Solid State Phys.* **13**, L851 (1980).